Available online at www.sciencedirect.com

ScienceDirect

IFAC Papers Online
CONFERENCE PAPER ARCHIVE

IFAC-PapersOnLine 49-8 (2016) 048–053

Boundary Feedback Control of Unstable thermoacoustic Oscillations in the Rijke Tube

Gustavo A. de Andrade * **Rafael Vazquez** ** **Daniel J. Pagano** *

* *Department of Automation and Systems, Universidade Federal de Santa Catarina, 88040-900, Florianópolis, SC, Brazil (e-mail: gustavo.artur@posgrad.ufsc.br, daniel.pagano@ufsc.br)*
** *Department of Aerospace Engineering, Universidad de Sevilla, Camino de los Descubrimientos, s.n.,41092 Sevilla, Spain (e-mail: rvazquez1@us.es)*

Abstract: The problem of boundary stabilization of thermoacoustic oscillations is investigated. The Rijke tube is used as prototype system to study such phenomena. We consider that this system is modelled as a 2×2 linear first-order hyperbolic system that behaves like a wave equation with the control variable at one boundary condition. Our control approach is based on employing characteristic coordinates to convert the system into a system of two delay elements. Analysing the periodicity of the solution of these equations a discrete transfer function is obtained. This enable us to employ a discrete time domain control design to guarantee the exponential stability of the closed-loop system. The performance of the controller is evaluated through simulation results.

Keywords: boundary control, method of characteristics, thermoacoustic instability, Rijke tube, stabilization

1. INTRODUCTION

In this paper, we investigate boundary stabilization of thermoacoustic oscillations in the Rijke tube. This phenomenon is described by high levels of sound produced by placing a heater release in a vertical tube with open ends. The mechanisms that cause unsteady heat release fluctuations are described in Lieuwen (2012). These instabilities also arise in combustors of gas turbines and aero engines in much more complex levels. These systems can oscillate in a self-excited way due to coupling between the unsteady heat release of a source and acoustic waves (generated by the pressure gradient).

This phenomenon is often modelled by the Euler equations of gas dynamics, where the control variable appears at one boundary condition (Epperlein et al., 2015). Remarkably, the Dirac delta distribution appears in the right hand side of these equations, implying in the discontinuity of the system states. Depending on the steady-state conditions about which these equations are linearized, the resulting linearization is a linear first-order partial differential equation (PDE) that behaves like a wave equation and thus describes acoustic wave propagation. The linearization of this model leads to the system considered throughout this paper.

Boundary stabilization of linear first-order PDEs has received significant attention in the literature, see for instance Vazquez et al. (2012); Di Meglio et al. (2013); Xu and Sallet (2014); Bastin et al. (2015); Aamo (2013); de Andrade and Pagano (2015) and the references therein. Unfortunately, these methods cannot be used in the system treated in this work, since the Dirac delta distribution is a non strict-feedback term [1].

Therefore, in this paper we propose a stabilizing state feedback control law based on the interpretation of the analytical solution of the system equations. We reformulate the system by introducing the characteristic coordinates, which allow us to convert the system equations to a system of transport equations which convect in opposite directions and reflects at the boundaries. As we shall see, in this framework a discrete transfer function of the system can be obtained by analysing the periodicity of the solution. Then, the control law is designed by using classical tools of discrete time domain systems, guaranteeing exponential stability of the zero equilibrium-point in the $\mathscr{L}^\infty$-norm. The proposed control strategy was tested via numerical simulations to show its effectiveness.

The paper is organized as follows. In Section 2, the Rijke tube and the mathematical model are described. The control design and the stability analysis of the closed-loop system with the proposed feedback control law are developed in Section 3. Simulation results are shown in Section 4. Finally, we discuss the obtained results and perspectives for future improvement in Section 5.

[1] The control methodologies in literature consider that the right hand side of the PDE system is given by bounded functions, which is not the case of the Dirac delta distribution. Therefore, for the Rijke system, a feedback control law cannot be directly obtained by applying these control strategies.

10.1016/j.ifacol.2016.07.417

2. THERMOACOUSTIC INSTABILITIES IN THE RIJKE TUBE

The Rijke tube experiment basically consists of a vertical tube opened in both ends and a heater source in the lower half. The air that traverses the heating zone expands, causing a sudden local pressure increase. The pressure propagates along the tube and reflect at the boundaries, ultimately influencing itself at the heating area. This property leads to a thermoacoustic coupling, which makes the system oscillates. A speaker placed at a slight distance under the tube is used as actuator, while a microphone placed near the top of the tube provides the pressure measurement. The diagram of the Rijke tube is depicted in Fig. 1.

The nonlinear model describing the dynamics of the gas inside the tube is given by the Euler equations:

$$\partial_t \rho + \partial_x(\rho v) = 0, \tag{1}$$

$$\partial_t(\rho v) + \partial_x\left(\rho v^2 + P\right) = 0, \tag{2}$$

$$\partial_t\left(\rho U + \frac{\rho v^2}{2}\right) + \partial_x\left(v\left(\rho U + \frac{\rho v^2}{2}\right) + Pv\right) = q, \tag{3}$$

$$P(t,0) = P_0 + u(t), \quad P(t,L) = P_0, \tag{4}$$

where $t \in [0, +\infty)$ is the time, $x \in [0, L]$ is the space, ρ is the gas density, P is the pressure, q is the external heat input, ρv is the momentum, v the velocity, u is the control input and P_0 is the ambient pressure. The internal energy is denoted by ρU. For a calorically perfect gas that also satisfies the ideal gas law, the internal energy is expressed by $\rho U = (c_v/R)/P$, where c_v is the specific heat capacity and R is the universal gas constant.

The external heat input is expressed by

$$q = \frac{1}{A}\delta(x - x_0)Q,$$

where δ is the Dirac delta distribution, Q is the heat power released from the coil and A is the tube cross section area. The heat release process, according to King's law, is modelled by

$$Q = l_w(T_w - T)(\kappa + \kappa_v\sqrt{|v(t,x_0)|}), \tag{5}$$

where l_w is the wire length, κ is the fluid thermal conductivity, κ_v is a empirical constant, and T_w and T are the wire and fluid temperature, respectively.

Using some algebra and the product rule of differentiation, system (1)-(3) is rewritten into the quasilinear form:

$$\partial_t \rho + v\partial_x \rho + \rho\partial_x v = 0, \tag{6}$$

$$\partial_t v + \partial_x v + \frac{1}{\rho}\partial_x P = 0, \tag{7}$$

$$\partial_t P + \gamma P \partial_x v + v\partial_x P = \overline{\gamma} q, \tag{8}$$

where $\gamma = 1 + R/c_v$, and $\overline{\gamma} = \gamma - 1$.

2.1 Equilibrium solutions and linearization

In this work, the steady-state solution for system (6)-(8) is assumed to be constant, i.e., $(\rho, v, P) = (\overline{\rho}, \overline{v}, \overline{P})$, $\forall t \in [0, +\infty)$, $\forall x \in [0, L]$. This hypothesis is valid because the important parameter in acoustic dynamics is the speed of sound, and the buoyancy effects as well as steady temperature and density variations along the tube length have relatively minor effect on the speed of sound.

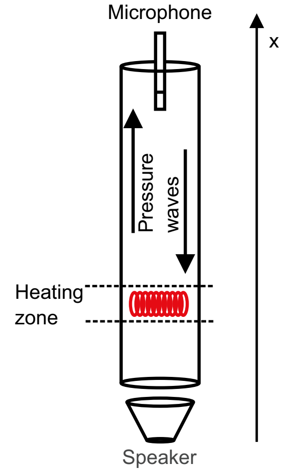

Fig. 1. Schematic of the Rijke tube with a heating element toward the bottom. The upward and downward arrows indicate the acoustic motion.

Another important remark about the system is that the flow satisfies the subsonic condition, i.e., $\overline{v} \ll c$, where $c = \sqrt{\gamma \frac{\overline{P}}{\overline{\rho}}}$ is the speed of sound.

In order to linearize the system (6)-(8) and its boundary conditions, we define the deviations of the states ρ, v and P with respect to the steady-states $\overline{\rho}$, $\overline{v}$ and $\overline{P}$ by

$$\tilde{\rho}(t,x) \triangleq \rho(t,x) - \overline{\rho},$$
$$\tilde{v}(t,x) \triangleq v(t,x) - \overline{v},$$
$$\tilde{P}(t,x) \triangleq P(t,x) - \overline{P}.$$

Then, the linearized model (6)-(8) around the steady-state is described by

$$\partial_t \tilde{\rho} + \overline{v}\partial_x \tilde{\rho} + \overline{\rho}\partial_x \tilde{v} = 0, \tag{9}$$

$$\partial_t \tilde{v} + \overline{v}\partial_x \tilde{v} + \frac{1}{\overline{\rho}}\partial_x \tilde{P} = 0, \tag{10}$$

$$\partial_t \tilde{P} + \gamma \overline{P}\partial_x \tilde{v} + \overline{v}\partial_x \tilde{P} = \frac{\overline{\gamma}}{A}\delta(x - x_0)\tilde{Q}, \tag{11}$$

where $\tilde{Q}$ is the linearized expression of (5). In addition, we consider an additional simplifying hypothesis on system (9)-(11): taking into account that the upward flow $\overline{v}$ is very small if compared to the speed of sound, it is easy to see that the contribution of $\overline{v}$ to the gas dynamics is negligible. Therefore, it is reasonable to set $\overline{v} = 0$, which results in the decoupling of the density equation (9) to the pressure and velocity dynamics, and then the density equation can be dropped from consideration. It follows that the linearization of the gas dynamics is given by

$$\partial_t \tilde{v} + \frac{1}{\overline{\rho}}\partial_x \tilde{P} = 0, \tag{12}$$

$$\partial_t \tilde{P} + \gamma \overline{P}\partial_x \tilde{v} = \frac{\overline{\gamma}}{A}\delta(x - x_0)\tilde{Q}. \tag{13}$$

Note that system (12)-(13) results on the wave equation with the heat fluctuations $\tilde{Q}$ as a source term at x_0.

Remark 2.1. We have to stress that the significance of the steady buoyancy-induced velocity $\overline{v}$ is different for the heat release than for the gas dynamics. In the gas dynamics, $\overline{v}$ only contributes in form of the steady-state and can be neglected. For the heat release (5), if the steady-state effect of the velocity is neglected, then the linearization would result invalid, since the derivative of $\sqrt{|\cdot|}$ is discontinuous at 0. The importance of considering $\overline{v} \neq 0$ in the heat release lies in moving to the differentiable part of the square root function.

In turn, the linearization of (5), considering $T = \frac{P}{\rho R}$, is given by

$$\tilde{Q} = f(\overline{v})\frac{\overline{T}}{\overline{\rho}}\tilde{\rho} + f'(\overline{v})(T_w - \overline{T})\tilde{v} - f(\overline{v})\frac{\overline{T}}{\overline{P}}\tilde{P}, \qquad (14)$$

where $f(\overline{v}) = l_w(\kappa + \kappa_v\sqrt{|\overline{v}|})$ and $\overline{T} = \overline{P}/(\overline{\rho}R)$.

The above equation shows the influence of each state variable on the heat transfer process. Performing a change of variable in $\tilde{v}$, $\tilde{\rho}$ and $\tilde{P}$, in order to turn them dimensionless quantities, it is possible to compare the size of the gain in the above equation [2]. This analysis shows that the velocity fluctuations are the main driver of the heat dynamics for subsonic flow. Therefore, it is reasonable to drop out the density and pressure fluctuations influence of (14), resulting in

$$\tilde{Q} \approx f'(\overline{v})(T_w - \overline{T})\tilde{v}.$$

Besides, the boundary conditions (4) linearized around an equilibrium point can be written as

$$\tilde{P}(t,0) = u(t), \qquad \tilde{P}(t,L) = 0. \qquad (15)$$

2.2 Model in terms of characteristic coordinates

In this section, we will reformulate the system (12)-(13) with boundary conditions (15) by introducing the characteristic coordinates. This result is presented in the following lemma, which can be easily proved by direct computation.

Lemma 2.1. Consider the invertible linear transformation $\mathbf{T} : \mathscr{L}^\infty(0, L)\times\mathscr{L}^\infty(0, L) \to \mathscr{L}^\infty(0, L)\times\mathscr{L}^\infty(0, L)$ such that

$$\begin{pmatrix}\tilde{v}\\ \tilde{P}\end{pmatrix} = \mathbf{T}\begin{pmatrix}R_1\\ R_2\end{pmatrix} = \begin{pmatrix}\dfrac{1}{2\sqrt{\gamma\overline{P}\overline{\rho}}} & -\dfrac{1}{2\sqrt{\gamma\overline{P}\overline{\rho}}}\\ \dfrac{1}{2} & \dfrac{1}{2}\end{pmatrix}\begin{pmatrix}R_1\\ R_2\end{pmatrix}.$$

The transformed linear system from (12)-(13) with boundary conditions (15) is written as follows

$$\partial_t R_1 + \lambda\partial_x R_1 = \beta\delta(x - x_0)\tilde{Q}_R, \qquad (16)$$
$$\partial_t R_2 - \lambda\partial_x R_2 = \beta\delta(x - x_0)\tilde{Q}_R, \qquad (17)$$
$$R_1(t,0) = -R_2(t,0) + 2u(t), \qquad (18)$$
$$R_2(t,L) = -R_1(t,L). \qquad (19)$$

with $\lambda = \sqrt{\frac{\gamma\overline{P}}{\overline{\rho}}}$, $\tilde{Q}_R = R_1 - R_2$ and $\beta = \frac{\overline{\gamma} f'(\overline{v})(T_w - \overline{T})}{2A\sqrt{\gamma\overline{P}\overline{\rho}}}$.

Note that in this new framework, the wave equation (12)-(13) is represented as two transport PDEs convecting in opposite directions at the speed of sound. The boundary conditions (18)-(19) account for the reflection of the wave at $x = 0$ and $x = L$, respectively.

2.3 Solutions and stability analysis

The solution of (16)-(19) can be obtained by applying the method of characteristics. To do that, we first restate these equations by changing the status of t and x, in order to obtain a solution parametrized w.r.t. space:

$$\frac{1}{\lambda}\partial_t R_1 + \partial_x R_1 = \frac{\beta}{\lambda}\delta(x - x_0)\tilde{Q}_R, \qquad (20)$$
$$\frac{1}{\lambda}\partial_t R_2 - \partial_x R_2 = \frac{\beta}{\lambda}\delta(x - x_0)\tilde{Q}_R. \qquad (21)$$

Consider any initial condition $(R_1^0, R_2^0)^T \in \mathscr{L}^\infty((0,L);\mathbb{R}^2)$ and define the characteristic curves $(\tau_1(t,x;\cdot), \tau_2(t,x;\cdot))$ corresponding to equations (20)-(21) as

$$\frac{d\tau_1}{ds}(x,t;s) = \frac{1}{\lambda}, \qquad s \in [0,L],\ \tau_1(x,t;0) = \tau_1^0,$$
$$\frac{d\tau_2}{ds}(x,t;s) = -\frac{1}{\lambda}, \qquad s \in [0,L],\ \tau_2(x,t;0) = \tau_2^0.$$

Then, integrating (20)-(21) along these characteristic lines and plugging the boundary conditions yields, for $t > \frac{L}{\lambda}$, in the following expressions:

- For $x < x_0$

$$R_1(t,x) = u^*\left(t - \frac{x}{\lambda}\right) \qquad (22)$$
$$R_2(t,x) = -R_1\left(t + \frac{x-L}{\lambda}, L\right) + \frac{\beta}{\lambda}\tilde{Q}_R\left(t + \frac{x - x_0}{\lambda}\right) \qquad (23)$$

- For $x \geq x_0$

$$R_1(t,x) = u^*\left(t - \frac{x}{\lambda}\right) + \frac{\beta}{\lambda}\tilde{Q}_R\left(t - \frac{x - x_0}{\lambda}\right) \qquad (24)$$
$$R_2(t,x) = -R_1\left(t + \frac{x-L}{\lambda}, L\right) \qquad (25)$$

where $u^*(t) = -R_2(t,\, 0) + 2u(t)$.

From the explicit solution shown above we have that, for $x \in [0, x_0)$, $R_1(t,\cdot)$ is a delay of its boundary condition, but at the point x_0 there is a jump (discontinuity) in the solution of R_1, which will propagate for $x \in (x_0, L]$ without change of shape. The same behavior occurs for R_2, but with opposite direction. As we shall see in the following proposition, the system can becomes unstable depending on the amplitude of this jump.

Proposition 2.1. Consider the system (16)-(18) with initial condition $(R_1^0,\, R_2^0)^T \in \mathscr{L}^\infty((0,L);\mathbb{R}^2)$. Then, if $u^*(t) = 0$, the zero equilibrium-point of (16)-(18) is unstable if $\frac{\beta}{\lambda} > 1$, stable if $\frac{\beta}{\lambda} < 1$ and neutrally stable if $\beta = \lambda$.

Proof. It is sufficient to concentrate our analysis in the behavior of the term $\tilde{Q}_R(t) = (R_1(t, x_0) - R_2(t, x_0))$ to conclude about the stability of (16)-(19). Notice that we can write $\tilde{Q}_R$ as a function of the boundary values, i.e.,

$$\tilde{Q}_R(t) = u^*\left(t - \frac{x_0}{\lambda}\right) + R_1\left(t + \frac{x_0 - L}{\lambda},\, L\right).$$

Using (24) and the fact that $u^*(t) = 0$ by hypothesis, the above equation is rewritten to

[2] Define $\tilde{m} \triangleq \tilde{v}/c$, $\tilde{r} \triangleq \tilde{\rho}/\overline{\rho}$, $\tilde{\psi} \triangleq \tilde{P}/\overline{P}$. Then, Eq. (14) rewritten to $\tilde{Q} = f(\overline{v})\overline{T}\tilde{r} + cf'(\overline{v})(T_w - \overline{T})\tilde{m} - f(\overline{v})\overline{T}\tilde{\psi}$. Comparing the gains of $\tilde{r}$, $\tilde{m}$ and $\tilde{\psi}$ leads to $\frac{f(\overline{v})\overline{T}}{cf'(\overline{v})(T_w - \overline{T})} = 2\frac{\overline{T}}{(T_w - \overline{T})}\left(\frac{\kappa}{\kappa_v\sqrt{\overline{v}}} + 1\right)\frac{\overline{v}}{c} \approx \frac{\overline{v}}{c}$. Therefore, the velocity fluctuations have, by a factor of approximately $\frac{\overline{v}}{c}$, greater influence on the heat transfer than the pressure and density.

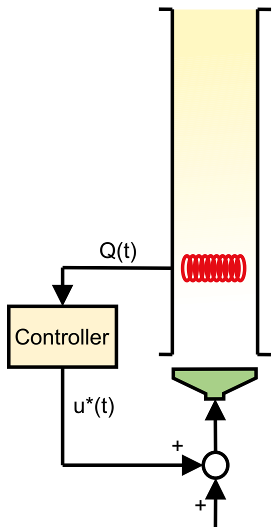

Fig. 2. Block diagram of the closed-loop system with the proposed control strategy. Note that this diagram has the only purpose of showing the variables used to calculate the control law. In the Rijke tube is not possible to directly measure $Q(t)$. 3.1 gives some comments to overcome this issue.

$$\tilde{Q}_R(t) = \frac{\beta}{\lambda}\tilde{Q}_R\left(t - 2\frac{L - x_0}{\lambda}\right). \tag{26}$$

From the above equation, it follows that the right hand side will decrease if $\frac{\beta}{\lambda} < 1$, and therefore the zero equilibrium-point of the system is asymptotically stable. On the other hand, if $\frac{\beta}{\lambda} > 1$, the right hand side of (26) will keep amplifying and therefore the zero equilibrium-point is unstable. In the special case where $\beta = \lambda$ the system is neutrally stable. This conclude the proof.

3. CONTROL DESIGN

In this section, we describe the proposed control system to stabilize the thermoacoustic phenomenon in the Rijke tube. Based on Proposition 2.1, we want to set u^*, such that $\tilde{Q}_R$ and u^* converge to zero as time grows. Then, the order of the transport speeds of system (16)-(17) yields that R_1 goes to zero and therefore R_2 goes to zero. Note that our design considers u^*, but ultimately the control law would be $u(t) = \frac{u^*(t)+R_2(t,0)}{2}$. The block diagram of the proposed control structure is illustrated in Fig. 2.

Remark 3.1. the proposed control strategy requires the measurement of the system states at the point x_0, which is not a realistic scenario since the Rijke tube is only equiped with a pressure sensor located near the top of the tube (see Section 2). Therefore, a state observer together with the control law would have to be used in practice.

For the proposed control strategy, we consider the following a priori assumption for the heat release position, which is typically fulfilled in practice.

Assumption 3.1. The heater position satisfies the inequality $x_0 < \frac{2}{3}L$.

As we shall see, this assumption is crucial to guarantee the causality of the proposed control system. If the assumption is not verified, it is possible to construct a more complex control law that stabilizes the system following a similar procedure.

In the following lemma, we present the open-loop discrete transfer-function between u^* and $\tilde{Q}_R$, which allow us to design the control law in the discrete time domain.

Lemma 3.1. Consider the system (16)-(19) and let z^{-1} be the delay operator associated with the sampling time $T_s = 2\frac{L-x_0}{\lambda}$. Then, the discrete transfer-function $G(z)$ relating u^* and $\tilde{Q}_R$ is given by

$$G(z) = \frac{1 + z^{-1}}{1 - \frac{\beta}{\lambda}z^{-1}}.$$

Proof. For sake of simplicity in the following calculations, define $\alpha = 2\frac{L-x_0}{\lambda}$. Note that for any $t = \tau + \frac{x_0}{\lambda}$, where τ is any fixed value in the closed interval $[0, \alpha]$, the expression of $\tilde{Q}_R$ can be written as

$$\tilde{Q}_R(\tau + (n+1)\alpha) = u^*\left(\tau - \frac{x_0}{\lambda} + (n+1)\alpha\right) + u^*\left(\tau - \frac{x_0}{\lambda} + n\alpha\right) + \frac{\beta}{\lambda}\tilde{Q}_R(\tau + n\alpha).$$

where $n \in \mathbb{N}$.

Define $u_n \triangleq \left(\tau - \frac{x_0}{\lambda} + (n+1)\alpha\right)$ and $\tilde{Q}_{R,n} \triangleq \tilde{Q}_R(\tau + (n+1)\alpha)$. Then, the above equation can be rewritten as a sequence with sampling time $T_s = \alpha$:

$$\tilde{Q}_{R,n} = \hat{u}^*_n + \hat{u}^*_{n-1} + \frac{\beta}{\lambda}\tilde{Q}_{R,n-1}. \tag{27}$$

Applying the Z-transform into (27) we obtain

$$\tilde{Q}_R(z) = u^*(z) + z^{-1}u^*(z) + \frac{\beta}{\lambda}z^{-1}\tilde{Q}_R(z),$$

or

$$G(z) = \frac{\tilde{Q}_R(z)}{u^*(z)} = \frac{1 + z^{-1}}{1 - \frac{\beta}{\lambda}z^{-1}}. \tag{28}$$

This concludes the proof.

Using the transfer function (28) we can apply a pole-placement design to fix a discrete controller $u^* = C(z)$ which give us:

- a stable closed-loop system $G_c(z) = \frac{G(z)}{1-G(z)C(z)}$;
- a stable controller response ($C(z)$ is stable).

In this work, we choose the controller structure $C(z) = \frac{az^{-1}}{1+bz^{-1}}$, where the controller stability condition is that b is inside the unit circle, i.e., $-1 < b < 1$. For this case, the closed-loop transfer-function is

$$G_c(z) = \frac{z^2 + (1+b)z + b}{z^2 + \left(b - \frac{\beta}{\lambda} - a\right)z - \left(a + b\frac{\beta}{\lambda}\right)}.$$

Then, supposing the desired closed-loop characteristic polynomial given by $(1 - kz^{-1})^2$, with $k \in (-1, 1)$, we can write a and b as

$$b = 1 - \frac{(k+1)^2}{\frac{\beta}{\lambda} + 1}, \qquad a = -\frac{(k - \frac{\beta}{\lambda})^2}{\frac{\beta}{\lambda} + 1}. \tag{29}$$

To guarantee the stability of C we need $b \in (-1, 1)$, and at the same time $k \in (-1, 1)$. But,

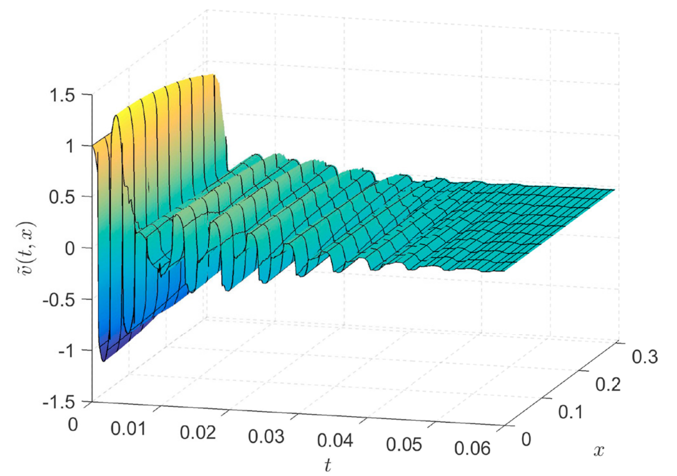

(a) Evolution of $\tilde{v}(t,x)$, for $x \in [0, x_0)$, under the boundary feedback controller.

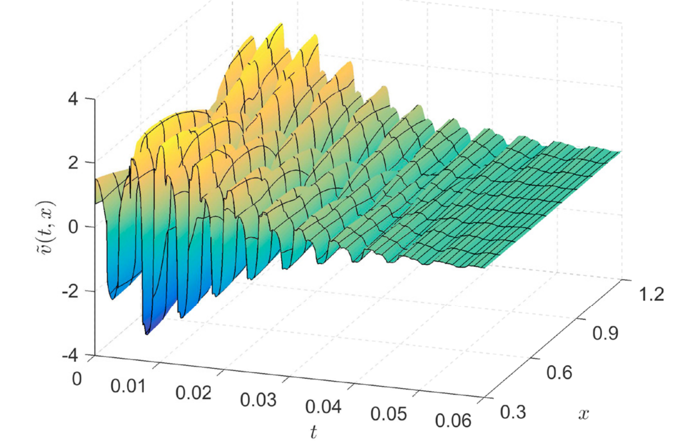

(b) Evolution of $\tilde{v}(t,x)$, for $x \in (x_0, L]$, under the boundary feedback controller.

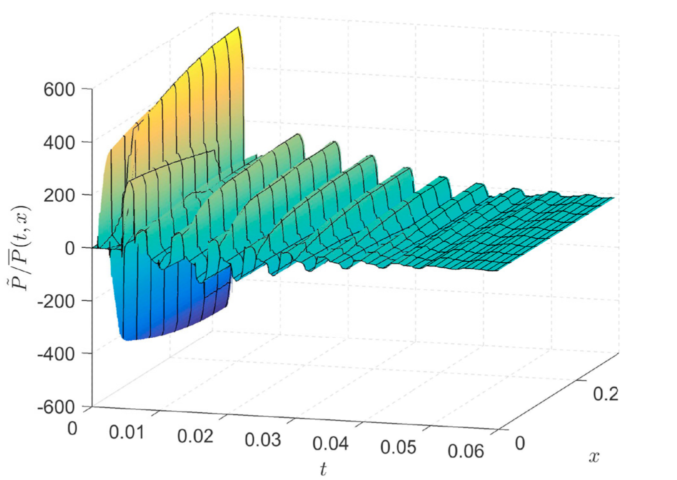

(c) Evolution of $\tilde{P}(t,x)$, for $x \in [0, x_0)$, under the boundary feedback controller.

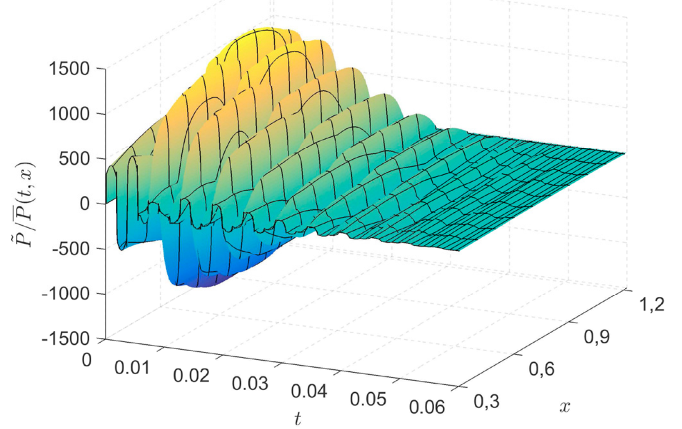

(d) Evolution of $\tilde{P}(t,x)$, for $x \in (x_0, L]$, under the boundary feedback controller

Fig. 3. Time evolution of the state profiles $\tilde{v}$ and $\tilde{P}$. The boundary feedback controller is turned on after $t = 0.0045$ s.

$$-1 < 1 - \frac{(k+1)^2}{\frac{\beta}{\lambda}+1} < 1 \Leftrightarrow -2 < -\frac{(k+1)^2}{\frac{\beta}{\lambda}+1} < 0.$$

Since $\frac{\beta}{\lambda} + 1 > 0$, then $-(k+1)^2 < 0$ is verified. In turn, the first inequality is reduced to $k < \sqrt{2(\frac{\beta}{\lambda}+1)} - 1$, which certainly can be satisfied by choosing k as close to -1 as necessary.

The control law is then

$$\hat{u}^*(z) = \frac{az^{-1}}{1+bz^{-1}}\tilde{Q}_R(z),$$

or

$$\hat{u}^*_n = -b\hat{u}^*_{n-1} + a\tilde{Q}_{R,n-1}, \tag{30}$$

which translates into

$$u^*(t) = \begin{cases} 0, & t < \alpha - \frac{x_0}{\lambda} \\ -bu^*(t-\alpha) + a\tilde{Q}_R\left(t - \alpha + \frac{x_0}{\lambda}\right), & t \geq \alpha - \frac{x_0}{\lambda}. \end{cases} \tag{31}$$

Remark 3.2. The control law (31) is causal if and only if $\alpha - x_0/\lambda$ is positive, i.e., $x_0 < \frac{2}{3}L$, which is satisfied thanks to the Assumption 3.1.

Remark 3.3. Note that the discrete transfer functions $G(z)$ and $C(z)$ are valid for any real value of $\tau \in [0, \alpha]$. Therefore using a continuity argument in τ we can translate the control law (30) to the continuous time domain (31), and consequently the analysis of stability of G_c in continuous time domain.

From the linear control theory, we have guaranteed that $\tilde{Q}_R(t) \to 0$ and $u^*(t) \to 0$ as $t \to \infty$. Therefore, using (22)-(25) to bound R_1 and R_2 in terms of u^* and $\tilde{Q}_R$, and from the stabilization properties of the control law, it is easy to show that there exist positive constants C, ν such that, for any initial condition $(R_1^0, R_2^0)^T \in \mathscr{L}^\infty((0,L);\mathbb{R}^2)$, the solution of (16)-(19), under the control law (31) satisfies

$$\| (R_1(t,\cdot), R_2(t,\cdot))^T \|_{L^\infty((0,L);\mathbb{R}^2)} \leq C\exp(-\nu t) \| (R_1^0, R_2^0)^T \|_{L^\infty((0,L);\mathbb{R}^2)} . \tag{32}$$

Table 1. Values of the parameters of the system.

Symbol	Description	Value
$\overline{\rho}$	Density	1.2 kg/m^3
$\overline{P}$	Pressure	10^5 N/m^2
$\overline{v}$	Velocity	0.5 m/s
γ	Adiabatic ratio	1.4
$\overline{\gamma}$	-	0.4
R	Ideal gas constant	290 J/(kg K)
L	Tube length	1.219 m
d	Tube diameter	0.0762 m
x_0	Heater position	$\frac{1}{4}L$
$\frac{\beta}{\lambda}$	-	1.1

With this result, we have proved the following theorem.

Theorem 3.1. Consider the system (16)-(19), with initial condition $(R_1^0, R_2^0)^T \in \mathscr{L}^\infty((0,L);\mathbb{R}^2)$ and under the control law (31), where $k \in (-1,1)$, and a and b are defined by (29). Then, there exist constants $C, \nu > 0$ such that the inequality (32) is satisfied.

4. SIMULATION RESULTS

This section shows the simulation results obtained when using the proposed controller to stabilize the linear model (16)-(19). To find the numerical solution of these equations, the HPDE solver for Matlab (Shampine, 2005) was used. The Rijke system parameters used in the simulation are shown in Table 1. Moreover, it was considered that the values of the states at the point x_0 are available for the control law, since the design of a state observer is out of the scope of this work. The control parameters are $k = 0.5$, $a = -0.17$ and $b = -0.07$.

Figures 3 and 4 depict the time domain simulation of the system with the proposed control law. At $t = 0.0045$ s, the control law was switched on. As can be seen the system converges asymptotically to zero as time goes to infinity after an initial overshoot.

5. CONCLUSIONS

In this paper we have addressed the issue of boundary feedback stabilization of thermoacoustic oscillations in the Rijke tube. Using characteristic coordinates allowed us to rewrite the system in a system of two delay elements. Interestingly, in this framework a discrete transfer function relating u^* and Q_R can be obtained by analysing the periodicity of the solution. Then, a control law based on the discrete time domain was proposed, where explicit sufficient conditions to achieve exponential stability in $\mathscr{L}^\infty$-norm have been provided.

Future works include the design of a state observer, which will allow us to consider an output-feedback controller. Moreover, we assumed that the heater position satisfies the inequality $x_0 < \frac{2}{3}L$. This assumption is crucial to guarantee the causality of the proposed control law. The general case will be covered in a future work.

Other directions of future work includes the improvement of the heating release model used in this work by adding a phase lag on its expression. The presented model can induces non-modeled sources of uncertainty in the control law when tested on practice. For this reason, further analysis is required to quantify the impact of modelling errors and the robustness of the proposed approach.

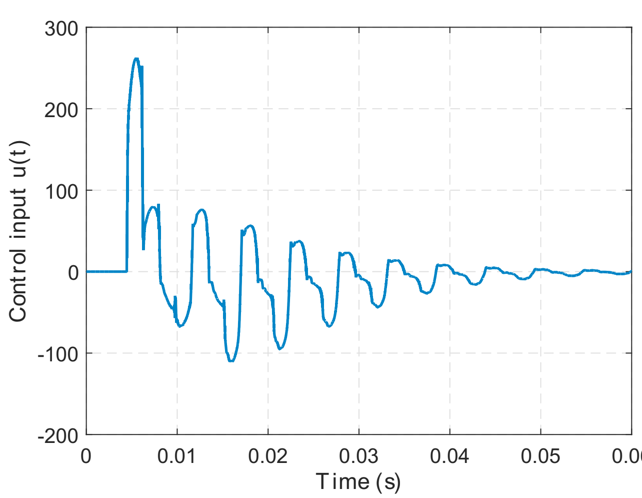

Fig. 4. Control input. The controller is turned on at $t = 0.0045$ s.

ACKNOWLEDGMENTS

Daniel J. Pagano and Rafael Vazquez acknowledge financial support of the Spanish Ministerio de Economía y Competitividad under grant MTM2015-65608-P. Gustavo A. de Andrade thanks the financial support given by the CNPq.

REFERENCES

Aamo, O.M. (2013). Disturbance rejection in 2×2 linear hyperbolic systems. *IEEE Transactions on Automatic Control*, 58(5), 1095–1106.

Bastin, G., Coron, J.M., and Tamasoiu, S.O. (2015). Stability of linear density-flow hyperbolic systems under PI boundary control. *Automatica*, 53, 37–42.

de Andrade, G.A. and Pagano, D.J. (2015). Boundary control for stabilization of slugging oscillations. In *Proceedings of the 2th IFAC Workshop on Automatic Control in Offshore Oil and Gas Production*, 77–82.

Di Meglio, F., Vazquez, R., and Krstic, M. (2013). Stabilization of a system of coupled first-order hyperbolic linear PDEs with a single boundary input. *IEEE Transactions on Automatic Control*, 58(12), 4097–3111.

Epperlein, J.P., Bamieh, B., and Astrom, J. (2015). Thermoacoustics and the Rijke tube: Experiments, identification and modeling. *Control Systems Magazine*, 35(2), 57–77.

Lieuwen, T.C. (2012). *Unsteady Combustor Physics*. Cambridge University Press.

Shampine, L.F. (2005). Solving hyperbolic PDEs in MATLAB. *Applied Numerical Analysis and Computational Mathematics*, 2(3), 346–358.

Vazquez, R., Krstic, M., and Coron, J.M. (2012). Collocated output feedback stabilization of a 2×2 quasilinear hyperbolic system using backstepping. In *Proceedings of the American Control Conference*, 2202–2207.

Xu, C.Z. and Sallet, G. (2014). Multivariable boundary PI control and regulation of a fluid flow system. *Mathematical Control and Related Fields*, 4(4), 501–520.